Characterisation and control platform for pneumatically driven soft robots: Design and applications

Jialei Shi[1], Wenlong Gaozhang[1], Hanyu Jin[1], Ge Shi[1] and Helge A. Wurdemann[1]

***Abstract*— Driven by performance criteria and requirements from specific applications in healthcare for instance, the soft robotics community have created a huge amount of different designs for pneumatically actuated soft robots. The assessment with regards to these criteria usually involves a full characterisation of the soft robotic system. In order to support these efforts during the prototyping phase and standardise assessment procedures, a physical platform is described in this paper that allows to gain essential insights into the characterisation and validation of control algorithms for pneumatically driven soft robots. The platform can be connected to a Matlab Graphical User Interface allowing to send pressure values as well as record and plot data, and, hence, it is able to actuate and characterise main features of soft robots, such as the kinematics/dynamics, stiffness and force capability. The user can chose between two control units including the NI USB-6341 and Arduino Due. These components facilitate implementing and validating control algorithms using different tools, e.g., Matlab/Simulink. To demonstrate the feasibility and functionalities of our platform, three soft robotic systems have been analysed. We present characterisation results for a variable stiffness joint, the kinematics results during the inflation of an elastic membrane and the validation of an open-loop control strategy for a soft continuum robot.**

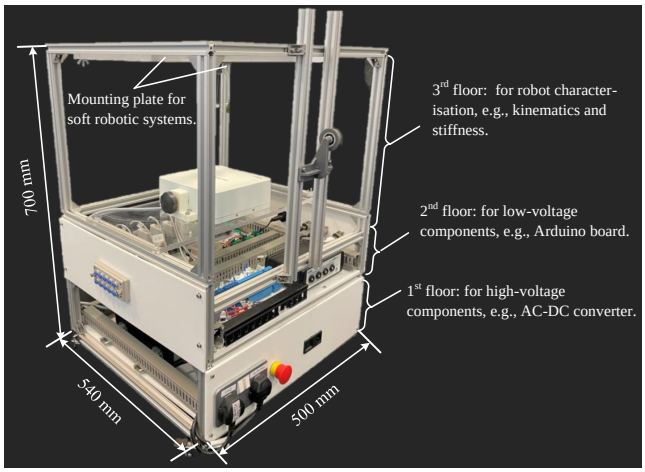

Fig. 1. Physical platform for actuation, characterisation (e.g., kinematics, stiffness and force identification), control implementation and validation of pneumatically driven soft robotic system. The platform consists of three floors covering high-voltage components, DC components and characterisation space. The CAD drawing in Fig. 4 gives a detailed view.

I. Introduction

Fluidically driven soft robotic manipulators can offer high flexibility and dexterity, a light-weight design and variable stiffness capability [1], [2]. Many robotic devices are pneumatically or hydraulically actuated pressurising cavities within soft material structures resulting in shape changes, e.g., ballooning, elongation or bending [3]. These type of robots have show benefits for various applications, e.g., for pick-and-place operations using soft grippers [4], for surgical interventions using soft robotic tools [5], [6], for rehabilitation using exoskeletons [7] and for industry using collaborative robots made of soft links and joints [8], [9]. These prototypes have been created with regards to the application's requirements, that have led to a variety of design methods, e.g., for inflatable manipulators or membranes [10], fibre-reinforcement structures [11], [12] and hybrid rigid-soft mechanisms [13]. To facilitate the prototyping and development process of these pneumatically driven soft robots, efforts towards generating standardised hardware and software tools have emerged. One example is the prominent 'Soft Robotics Toolkit' [14].

The initial step of creating a physical soft robotic prototype concerns the fabrication technique. Aiming at providing and generalising a design paradigm for creating fluidically driven robots, a fabrication recipe is presented in [3]. Some challenges in the state-of-the-art method of manufacturing soft robotic systems remain, including enhancing the manufacturing accuracy and consistency [15]. Any kinematic change and dynamic behaviour results from the change in input air pressure. Hence, the development of soft robotic systems have not only focused on the robot design but also on valves and pressure regulators, that form essential actuation components. Advancements in actuation systems include the Programmable-Air platform [16], PneumaticBox [17], Penuduino [18], addressable regulators [19], OpenPneu [20] and FlowIO [21]. For instance, the recently launched FlowIO aims to supply air actuation through a miniaturised, portable and self-contained system. A desktop-size actuation system has been developed in [22], which can be used for real-time control applications. The device is compatible with MATLAB/Simulink. Similarly, a control and drive system (PneuSoRD) for soft robots is presented in [23], to control the pressure using on-off and proportional valves via Simulink or LabVIEW. Furthermore, interdisciplinary research has focussed on pressurised fluids by using chemical means [24], purposed mechanisms [25] and soft materials [26].

This work is supported by the Springboard Award of the Academy of Medical Sciences (grant number: SBF003-1109), the Engineering and Physical Sciences Research Council (grant numbers: EP/R037795/1, EP/S014039/1 and EP/V01062X/1), the Royal Academy of Engineering (grant number: IAPP18-19\264), the UCL Dean's Prize, UCL Mechanical Engineering, and the China Scholarship Council (CSC).

[1]J. Shi, W. Gaozhang, H. Jin, G. Shi and H.A. Wurdemann are with the Department of Mechanical Engineering, University College London, UK. h.wurdemann@ucl.ac.uk

In addition to the hardware development, frameworks for kinematics/dynamics modelling and control algorithms have been created. Examples include the piecewise constant curvature and the Cosserat rod model [27], [28]. Based on these models, (openly accessible) software tools have been proposed and are available to the soft robotics community [29]. For instance, the Simulation Open Framework Architecture (SOFA) has been created, which can deliver physical simulation and real-time control for soft robots using Finite Element Method (FEM) [30]. Further frameworks include SoRoSim based on Matlab achieving modelling and control of soft or hybrid rigid-soft robotic systems based on the geometric variable strain model [31]. Sorotoki is a Matlab toolbox that offers the ability to design, model, and control soft robots, using the FEM and geometric theory [32]. To allow users to customise design parameters for bellow soft pneumatic bending actuators, a Matlab toolbox was designed in [33], which can generate CAD files and then simulate the actuators' performance using analytical or FEM models.

Overall, tremendous advances have been made in sharing tools for soft robot manufacturing and fabrication, on pneumatic actuation systems, modelling and control algorithms. The available packages have significantly supported soft robotic development, in addition to, motivating relevant research. On the other hand, Joshi and Paik [34] have made progress towards a platform to characterise forces of a soft manipulator. However, a combined physical testing platform, which consists of an actuation system and, at the same time, which is able to fully characterise the performance of soft robotic systems during the prototyping process, could be beneficial to validate modelling and control algorithms.

In this paper, we present the design of a characterisation platform, which includes air pressure actuation, evaluation of kinematics/dynamics, stiffness/compliance and force capability, as well as control validation, for pneumatically actuated soft robotic systems. The feasibility of our platform is demonstrated through the analysis of a number of soft robotic prototypes. In particular, we first discuss required functionalities of our platform to characterise soft robotic systems. We then present the physical platform and detail its structure and design. A graphical user interface (GUI) is designed to facilitate the usage of the platform. Finally, we provide three showcase studies, including the characterisation of soft inflatable membranes, a rigid-soft pneumatic-driven joint, and inverse kinematics control of a soft continuum robot. The design of the platform and related Simulink examples are accessible via the GitHub repository: https://github.com/ucl-robotics-ai/test-platform-soft-robotics.

This remainder of the paper is structured as follows: The requirements of the proposed platform for soft robotic systems characterisation are discussed in Section II. Section III describes the platform design, including the hardware, i.e., structure and electronic design, and the software, a GUI toolbox for robot characterisation. Section IV then reports on three use cases demonstrating the feasibility of the platform. The discussion and conclusions are then presented in Section V.

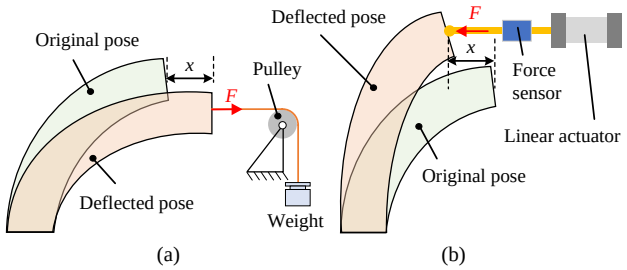

Fig. 2. Stiffness measurement demonstrated on a soft robotic manipulator applying (a) a pulling and (b) a pushing force. The force F results in a displacement or deflection x along the force direction.

II. Requirements for Characterisations of Soft Robots

This section highlights the requirements for the characterisation of soft robotic systems, e.g., with regards to the kinematics/dynamics, stiffness and force capability. Theses considerations then guide the platform design.

A. Kinematics, Dynamics and Motion Tracking

Motion tracking is of paramount importance for the kinematic/dynamic characterisation and control of soft robots. This data is essential for evaluating robot's performance during prototyping stages and implementing control strategies, e.g., for curvature [28] or task space regulation [35]. The actuation variables and robot motion needs to be monitored. Motion tracking can be achieved using 3D tracking systems (e.g., by OptiTrack) or electromagnetic trackers (e.g., by Northern Digital Inc. (NDI)). For instance, a 6-DoF sensor from the NDI Aurora magnetic tracking system can provide both position and orientation information.

B. Stiffness/Compliance Identification

Compliant materials used to fabricate soft robotic systems provide flexibility and adaptability. Understanding the stiffness of soft robots is critical for the robot's design, e.g., determining suitable materials and morphology for targeted applications. To quantify the value of softness, stiffness or the inverse, compliance, is often determined. As this value depends on force and displacement measurements, a load cell could either push or pull at different locations of a soft robot (e.g., at a manipulator's tip), as shown in Fig. 2.

A pulling force could be used to achieve stiffness identification (see Fig. 2(a)). A tendon is attached to the tip of a

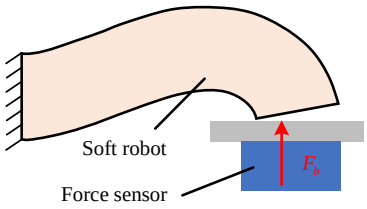

Fig. 3. Example of a blocked force identification setup. The tip of the robot is locally constrained when the robot is actuated. The force F_b can be measured by a force sensor.

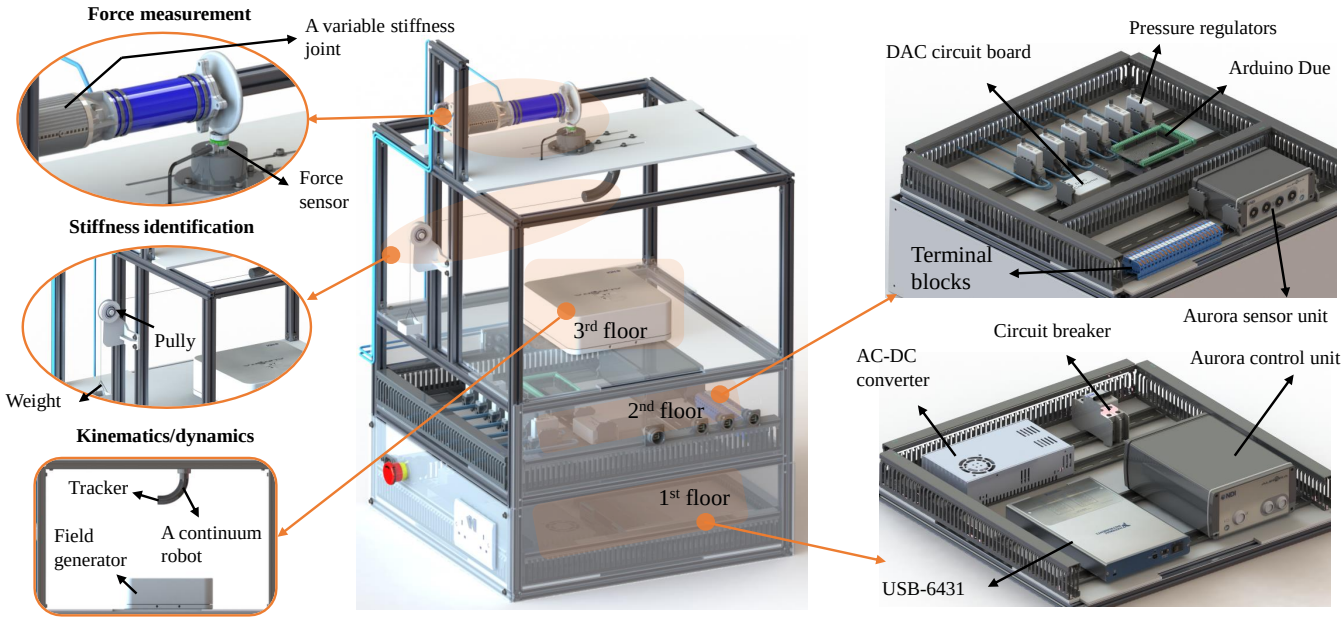

Fig. 4. Detailed hardware structure of our characterisation and control platform. The platform is able to validate kinematics/dynamics models through motion tracking, identify stiffness and measure blocked forces as discussed in Section II (as shown on the left hand side). The first floor includes an AC-DC converter, circuit breaker, the multifunction I/O device USB-6431, and the Aurora control uni. The second floor is made of the DAC cicuit board, Arduino Due, terminal blocks and pressure regulators. The third floor includes the field generator of the Aurora magnetic tracking system and a mounting plate for soft robotic systems. The CAD files are available in the GitHub repository.

soft robot on the one side and pulled by a calibrated weight in the other side. In this case, any friction and measurement errors of the force could be mitigated. The displacement x would need to be monitored by tracking devices.

When measuring the stiffness by a pushing force (see Fig. 2(b)), a force transducer is mounted on a linear rail [8] or robotic arm [36] exerting a force on the soft robot resulting in a displacement x. This method has been extensively applied to characterise soft robotic manipulators [3], [36]. It is worth mentioning that any friction between the robot and sensor is inevitable. In particular, when the measured force values are relatively small [37], any unexpected friction force errors could significantly influence readings. In comparison, the stiffness identification by pulling forces might have higher accuracy compared with pushing forces, which can be advantageous for stiffness or compliance model validation [38].

C. Force Identification

For robots that physically interact with the environment, it would be beneficial to understand the soft robot's behaviour when contact forces are exerted [3], [4]. In this case, the blocked force can be used to describe the force capability of the robot. To achieve this, a force sensor could be added to constrain the robot's tip in a certain pose. The robot might deform generating an interaction force. The force sensor could measure, e.g., this blocked force at the tip.

In summary, the functionality of our characterisation platform should include the above mentioned features. Our platform should be able to accommodate the characterisation of various soft robotic systems.

III. System Overview and Platform Design

Following the identification of the desired features in Section II, this section will present the details on the design of the platform and its interface. The overall structure of the platform is shown in Fig. 4, with its electrical architecture shown in Fig. 5. The platform can be connected to a GUI toolbox for robot characterisation (see Fig. 6).

A. Hardware Overview and Design

The platform contains: six proportional valves (Camozzi K8P) to regulate pneumatic air pressure; an electromagnetic tracking system (NDI Aurora) to monitor the position and orientation of a robot; a force/torque (F/T) sensor (IIT-FT17) to achieve force identification; electronic circuits to regulate proportional valves; a control unit (i.e., a USB-6341 and an Arduino Due) and a 220V AC power supply to power the platform. The multifunction I/O device USB-6341 (National Instruments) and an Arduino Due form the control unit, which can be selected based on the application. The Arduino Due has a 32-bit 84MHz processor, 512 KB flash memory, up to 12 PWM outputs and 12 analogue inputs (12-bit). On the other hand, the USB-6341 offers high frequency acquisition (up to 500 k Sample/s) and is equipped with up to 16 analogue inputs and 24 digital outputs (including 4 PWM ports).

The high-voltage (220V AC) and low-voltage ($\leq$ 24V DC) components are positioned on different floors to ensure electrical safety. The top floor is designed for accommodating different characterisation setups (as described in Section II). The structure of the platform can be divided into:

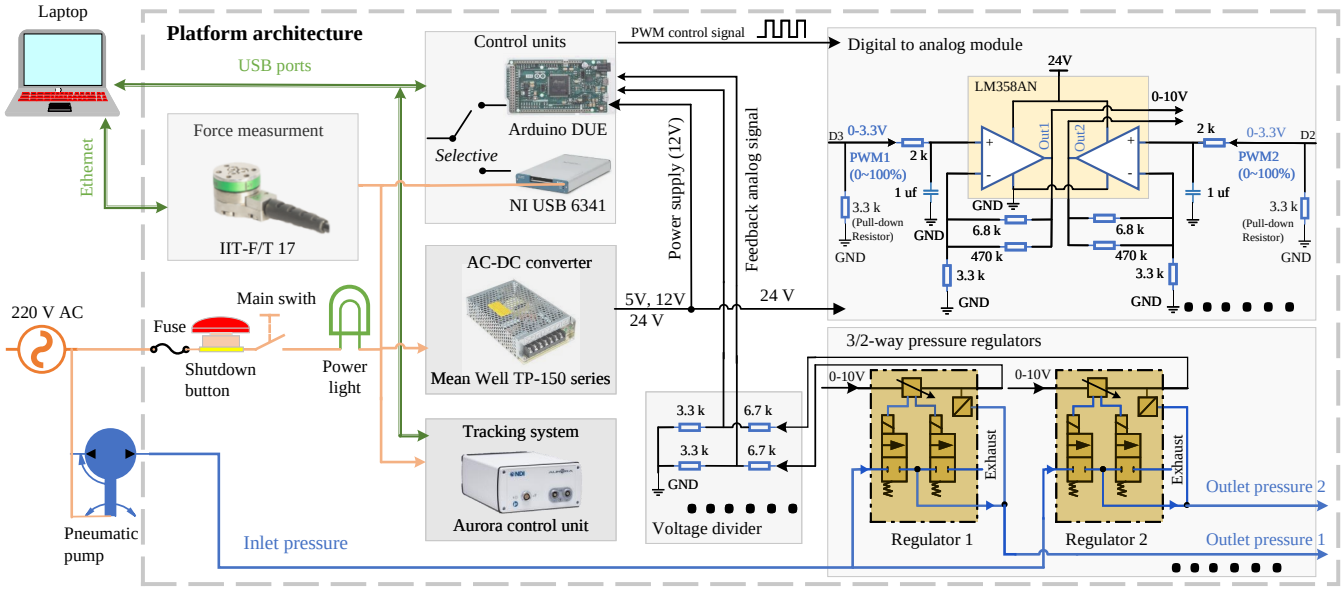

Fig. 5. Connection architecture of the platform. AC power and inlet pressure are provided from external supplies. Data transmission between the laptop and the platform is achieved via USB and Ethernet. Both the Arduino Due and USB-6341 can be selected as the control unit, depending on specific applications.

The first floor includes components in need of 220V AC power, i.e., the NDI Aurora, F/T sensor and USB-6341. In additional, an AC-DC converter (Mean Well TP-150D, 154 W) provides 5V (2∼20A), 12V (0∼1 A) and 24V (0.4∼4A) DC voltage for low-voltage DC electronics. Protection circuits, including a emergency shutdown button (Schneider Harmony XB5) and over-current fuse (Allen Bradley 1492-SPM, 6A), are embedded to ensure safety.

The second floor is dedicated to low-voltage ($\leq$ 24V DC) electronic circuits. Six pressure regulators can be used to control and monitor chamber pressures within soft robotic systems (0∼3 bar, 6 L/min). Pressurised air is supplied to the regulators by a HYUNDAI HY5508 compressor. The regulators are controlled by a 0∼10V analogue voltage, which are converted from PWMs generated by the Arduino Due or USB-6341. To achieve Digital-to-Analogue Conversion (DAC), the PWM is first filtered by a resistor-capacitor (RC) circuit (time constant τ =2 ms). The output is then amplified by non-inverting Op-Amps (Texas Instruments LM358AN/NOPB, dual supplies). The amplifier gain k_a depends on the voltage levels of the control units, e.g., k_a is 3.03 for the Auduino Due (shown in Fig. 5) and 2 for the USB-6341. For each PWM output port, a pull-down resistor (3.3 kΩ) is connected to have a default zero output when there is no PWM output value. As such, the PWM duty is proportional to the converted analogue signal and used to control the pressure regulators. The pressure regulators can also monitor the pressure via an analogue output ($0 \sim 10$V). It is worth mentioning that the feedback voltage needs to be processed by a voltage divider to make it compatible for the Arduino Due. Details of the electrical design can be found in Fig. 5. All wire connections are integrated through screw clamp terminal blocks.

The third floor is used to achieve the evaluation and characterisation of soft robots, e.g., kinematics/dynamics, stiffness and force identification. For motion tracking, the field generator of the NDI Aurora electromagnetic tracking system is located at the bottom of the floor to provide an electromagnetic domain, so the system can track the robot motion by attached trackers. The force sensor can be positioned to achieve a force-related identification.

B. Communication Interface and GUI Toolbox Design

The platform provides the opportunity for versatile programming and communication interfaces. All devices are connected to a host computer via USB and Ethernet. The software package LabVIEW, for instance, is compatible with the NI USB-6341 providing mature libraries to facilitate programming. In addition, MATLAB's DAQ toolbox can be connected to the NI devices through embedded MATLAB libraries. Compared to the USB-6341, the Arduino Due offers more flexibility and advantageous, e.g., for self-defined serial port communication. It either can be programmed using Arduino code or a third-party software provider, e.g., MATLAB/Simulink, with Arduino support packages. This is beneficial for real-time control implementation and tuning parameters in a cost-efficient and convenient way.

To facilitate the characterisation of soft robotic systems in line with the discussions in Section II, a user-friendly GUI toolbox has been designed in the Matlab. A snapshot is shown in Fig. 6(a). The architecture of the GUI is presented in Fig. 6(b). In this GUI, users need to first select different modes/functions (see Fig. 6(a)) from the main setting page, based on the characterisation requirements. Three sub-pages are designed to achieve different functions and save the results. In particular, these functions include:

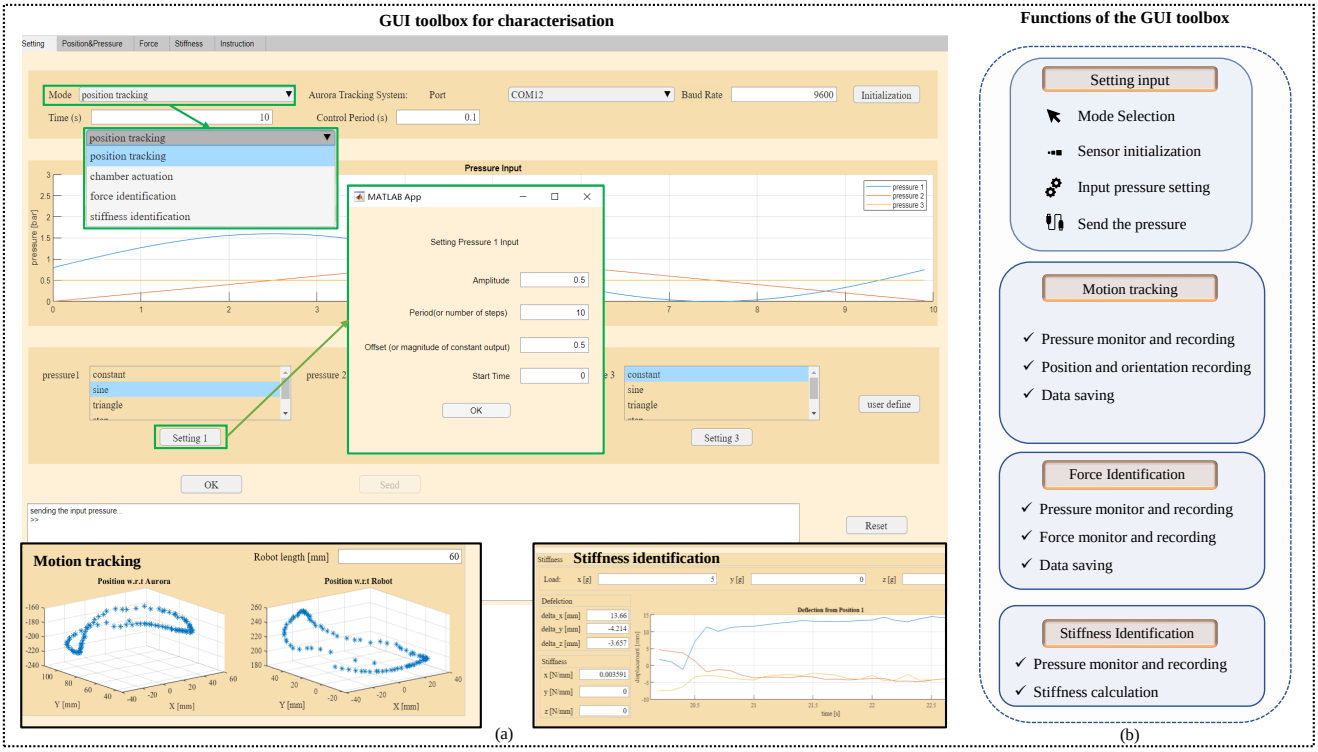

Fig. 6. The design of the GUI toolbox for robot characterisations. (a) Snapshots of the main page for setting, with the motion recording and stiffness identification examples shown at the bottom. (b) The architecture of the GUI. The source codes for the GUI can be downloaded from the GitHub repository.

1) Chamber actuation: In this mode, a user is able to test the robotic system using default (e.g., sine-wave, step) or user-defined pressure inputs. Pressure values can be controlled and monitored.
2) Position tracking (in line with Section II-A): This mode is for kinematics/dynamics evaluation. After an actuation pressure value has been inserted, the corresponding results can be recorded and saved.
3) Stiffness identification (in line with Section II-B): The change in displacement can be measured and recorded by the tracking system for an applied known load. As such, the stiffness is calculated.
4) Force identification (in line with Section II-C): In this mode, the force capability is identified..

IV. Characterisation Examples of Soft Robotic Systems

Three soft robotic systems are used as use cases to demonstrate the platform's functionality. A stiffness-controllable joint, an inflatable membrane and a soft continuum robot are analysed and characterised.

A. Characterisation for a Stiffness-controllable Joint

The first use case involves a variable stiffness joint for collaborative robots achieving inherently safe human-robot interaction. The joint is made of two elements: a rigid central hinge, and two silicone chambers with fibre reinforcement located on two sides of the hinge. The pressure difference between two chambers results in the robot to bend clockwise or anti-clockwise. At the same time, the antagonistic actuation of the two chambers can be used to change the stiffness of the joint.

The characterisation of the joint's bending angle, output force and variable stiffness capability was conducted using our platform. When identifying the bending angle and stiffness, the variable stiffness joint was mounted upside down onto the plate on the third floor of the platform. A 6-DOF aurora tracker was attached at the tip of the joint to measure the variation of the bending angle. When identifying the force generation, the joint was mounted with the force sensor, onto the same plate of the platform (see Fig. 4).

Fig. 7 shows the results from the GUI toolbox. In Fig. 7(a), the loading (red curve) and unloading (blue curve) bending behaviour of the joint is recorded when it was linearly actuated from 0 to 3 bar pressure. The maximum bending angle reaches around 45°. It is observed the hysteresis of the loading and unloading curves is non-negligible, e.g., the maximum angle difference of the two curves is 9.1°, i.e., 20.5% with respect to the maximum bending angle. The results for the blocked force measurements are shown in Fig. 7(b). Again the loading and unloading curve is plotted. The test results that the joint can achieve around 19 N output force when it was actuated by 1.5 bar air pressure, and the hysteresis is barely observed. Lastly, the platform can also be used to evaluate the stiffness of the joint. In this case, two stiffness values have been generated by the following chamber combinations: 0.1/0.46 bar and 0.35/0.65 bar. Both

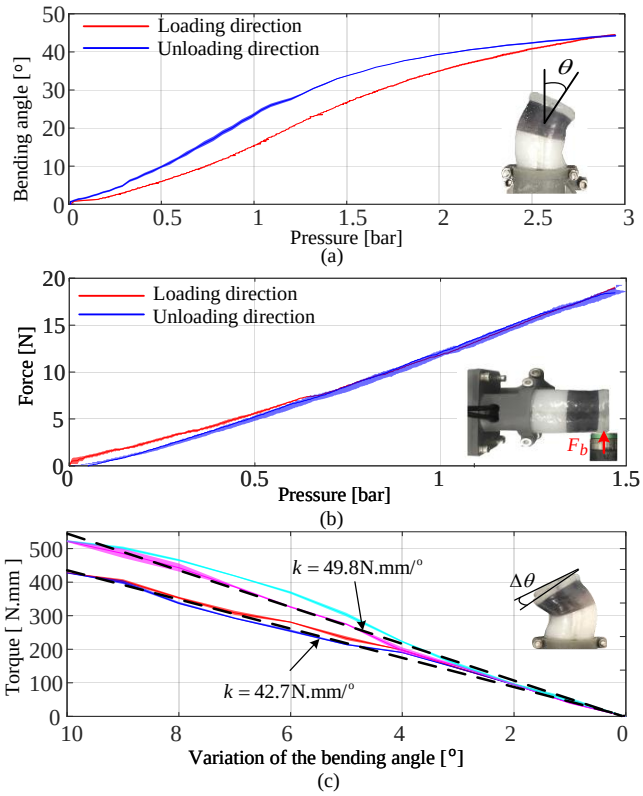

Fig. 7. Characterisation results for the variable stiffness joint. (a) Kinematics identification. (b) Force generation identification. (c) Variable stiffness analysis for two pressure combinations.

pressure combinations result in the same bending angle of 20°. The results in Fig. 7(c) show that the joint can achieve an increase in stiffness from 42.7 N.mm/° to 49.8 N.mm/°, by changing the pressure combination.

B. Measurement of Inflation Height of an Elastic Membrane

The inflation of soft elastic membrane is common in soft robots [10] and haptics [39]. In order to return desired deformations or force responses from an elastic membrane under a certain pressure, the characterisations of membranes are required for specific applications. Our designed platform is able to analyse this behaviour. The elastic membrane has been fixed to the characterisation floor and pressurised for characterising the relationship between pressure and inflation height. During the experiment, a load of 50 g and 100 g were exerted to the membranes. The inflation height h_0 of the pressurised membrane has been monitored using the Aurora tracker as well as the applied pressure values. Hence, the relationship between the inflation height and actuation pressure has been identified under different load conditions. Fig. 8 shows the results of characterising a circular elastic membrane with a load of 50 g in red colour and 100 g in blue colour. The figure reports on the standard deviation and also compares the experimental data with a computational model. The curves suggest a highly linear behaviour for pressure vs height between 0 and 0.1 bar pressure.

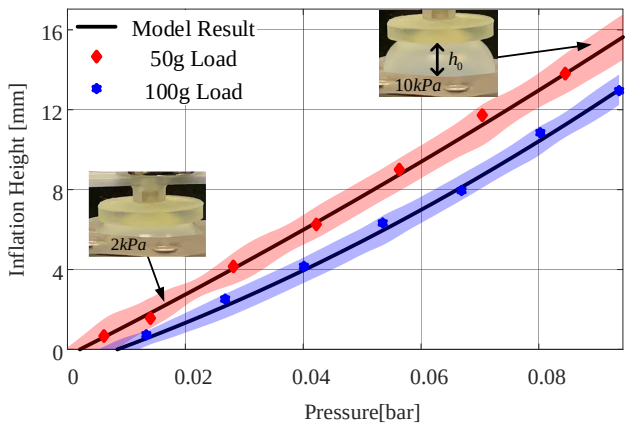

Fig. 8. Results for an inflation of a circular elastic membrane with constant load of 50 g and 100 g.

C. Inverse Kinematics Control for a Soft Continuum Robot

For the third use case, a soft robotic manipulator is mounted to our platform. The manipulator is made of a cylindrical silicone body with three fibre-reinforced chamber pairs that can be pneumatically pressurised. Applying pressure in one or two chamber pairs will lead to bending behaviour; pressurisation of all chambers simultaneously will achieve elongation [40]. The cross-sectional geometry of the robot used in our experiment is the same as Type-1 robot reported in [37]. The diameter of the robot is 14.5mm and the length is 60 mm.

To analyse a control implementation, Simulink is used for open-loop inverse kinematics control based on the Cosserat rod model. The spatial configuration of the robot's backbone, including the displacement vector $p(s)$ and the rotation matrix $R(s)$, can be differentiated with respect to the curve length s, where $\partial(\cdot)/\partial s$ denoted by $(\cdot)_{,s}$. Eqn. (1) yields.

$$p_{,s}(s) = R(s)v(s), \quad R_{,s} = R(s)\hat{u}(s), \tag{1}$$

where $v(s)$ is the local strain vector and $u(s)$ is the local curvatures and torsion. In addition, the derivatives of force $n(s)$ and moment $m(s)$ can be described by (2).

$$n_{,s}(s) = f_e(s) + f_P(s), \; m_{,s}(s) = -\hat{p}_{,s}n(s) - l_e(s) + l_P(s), \tag{2}$$

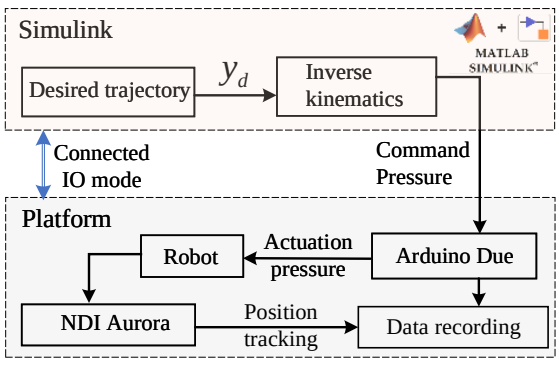

Fig. 9. Control scheme of implementing the inverse kinematics to the platform using Simulink.

where $f_e(s)$ and $l_e(s)$ are the distributed external force and moment. $f_P(s)$ and $l_P(s)$ are the distributed force and moment resulting from pressurisation. More details can be found in [29]. A linear constitutive material model is adopted to relate $n(s), m(s)$ to $v(s), u(s)$ yielding in (3).

$$n(s) = R(s)K_{se}(v(s) - [0,0,1]^T), m(s) = R(s)K_{bt}u(s), \quad (3)$$

where K_{se} contains the shear and elongation stiffness, and K_{bt} contains the bending and torsion stiffness [27]. To achieve trajectory tracking, the shooting method is used. The initial guess $g(0)$ is set as in (4).

$$g(0) = [n(0), m(0), P_1, P_2, P_3], \quad (4)$$

where $n(0)$ and $m(0)$ are the force and moment at the base, and P_1, P_2, P_3 are the desired actuation pressure in three chambers. When the robot has no interaction with the environment, the boundary conditions are as written in (5).

$$n(L)^b = F_P^b, \; m(L)^b = m_P^b, \; p(L) = y_d, \quad (5)$$

where superscript b denotes the body frame. As such, F_P^b and m_P^b are the force and moment written in the body frame and resulting from the pressurisation. y_d is the desired position. The inverse kinematics is achieved by integrating (1) and (2) based on the initial condition (4). The levenberg-marquardt optimisation can update the initial guess until the boundary condition in (5) satisfies.

Simulink is used to implement the inverse kinematics The command pressure is sent to the platform via an USB port. Simulink runs in the Connected IO mode. The control scheme is shown in Fig. 9. Figs. 10(a), (c) and (e) show the tracking results for circle, rectangle and heart shapes recorded by the Aurora magnetic tracking system. Figs. 10(b), (d) and (f) report the collected corresponding actuation pressure. Desired information, e.g., position and actuation pressure values, can be recorded for further analysis. Apart from the control implementation, it is worth mentioning that the characterisation showcases for this manipulator can also be found in [37] for kinematics, and [41] for dynamics.

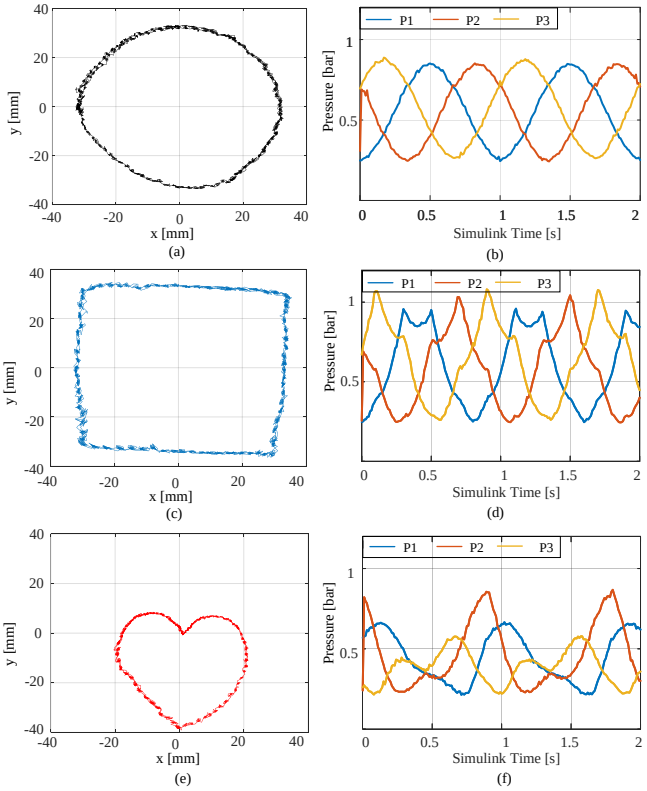

Fig. 10. Results for the inverse kinematics implementation. The Aurora tracking system records the different trajectories of (a) a circular, (c) a rectangular and (e) a heart shape. The recorded control pressure values are plotted in (b), (d) and (f). This Simulink example can be downloaded from the GitHub repository.

V. Conclusions

This paper presents the design of a physical platform supporting the actuation, characterisation and control implementation/validation for pneumatically driven soft robotic systems. Firstly, we summarised the functionality requirements for the characterisation of soft robots with regards to their kinematics/dynamics, force and stiffness identification. To fulfil these functions, we described the structure and electronics design of the platform in detail. At the same time, a Matlab GUI toolbox has been created to facilitate and streamline a soft robot's characterisation process. The functionality of the platform was validated by three use cases, including the characterisation of a variable stiffness, hybrid rigid-soft joint, an elastic membrane and the inverse kinematics control implementation of a soft continuum robot via Simulink.

In line with efforts of the soft robotic community to support the design of soft robotic systems, e.g., in [16]–[19], [21] and the development of the modelling and control algorithms from [30]–[33], the combination of our platform with a GUI toolbox provides a solution to characterise soft robots' performances during the prototyping stage and to further build a validation bridge between the development of modelling algorithms and robot prototyping. The design is made freely available to potentially support the soft robotics community. In this sense, we focused on the functionality of the platform and aimed to build in off-the-shelf components to standardise the list of components and ensure the stability of the system.

In future, we aim to advance the capability of our platform through integration into the Robot Operating System. Furthermore, we will make the use of the remaining available I/Os and increase the controllable pneumatic channels.

References

[1] D. Rus and M. T. Tolley, "Design, fabrication and control of soft robots," *Nature*, vol. 521, no. 7553, pp. 467–475, 2015.

[2] J. Peters, E. Nolan, M. Wiese, M. Miodownik, S. Spurgeon, A. Arezzo, A. Raatz, and H. A. Wurdemann, "Actuation and stiffening in fluid-driven soft robots using low-melting-point material," in *2019 IEEE/RSJ International Conference on Intelligent Robots and Systems (IROS)*, 2019, pp. 4692–4698.

[3] A. D. Marchese, R. K. Katzschmann, and D. Rus, "A recipe for soft fluidic elastomer robots," *Soft robotics*, vol. 2, no. 1, pp. 7–25, 2015.

[4] Sachin, Z. Wang, and S. Hirai, "Analytical modeling of a soft PneuNet actuator subjected to planar tip contact," *IEEE Transactions on Robotics*, pp. 1–14, 2022.

[5] H. Abidi, G. Gerboni, M. Brancadoro, J. Fras, A. Diodato, M. Cianchetti, H. Wurdemann, K. Althoefer, and A. Menciassi, "Highly dexterous 2-module soft robot for intra-organ navigation in minimally invasive surgery," *The International Journal of Medical Robotics and Computer Assisted Surgery*, vol. 14, no. 1, p. e1875, 2018.

[6] K.-W. Kwok, H. Wurdemann, A. Arezzo, A. Menciassi, and K. Althoefer, "Soft robot-assisted minimally invasive surgery and interventions: Advances and outlook," *Proceedings of the IEEE*, vol. 110, no. 7, pp. 871–892, 2022.

[7] P. Polygerinos, Z. Wang, K. C. Galloway, R. J. Wood, and C. J. Walsh, "Soft robotic glove for combined assistance and at-home rehabilitation," *Robotics and Autonomous Systems*, vol. 73, pp. 135–143, 2015.

[8] A. Stilli, H. A. Wurdemann, and K. Althoefer, "A novel concept for safe, stiffness-controllable robot links," *Soft Robotics*, vol. 4, no. 1, pp. 16–22, 2017.

[9] J. Fras, Y. Noh, H. Wurdemann, and K. Althoefer, "Soft fluidic rotary actuator with improved actuation properties," in *2017 IEEE/RSJ International Conference on Intelligent Robots and Systems (IROS)*. IEEE, 2017, pp. 5610–5615.

[10] N. Herzig, J. Jones, E. Perez-Guagnelli, and D. D. Damian, "Model and validation of a highly extensible and tough actuator based on a ballooning membrane," in *2021 IEEE International Conference on Robotics and Automation (ICRA)*, 2021, pp. 11 961–11 967.

[11] K. Suzumori, S. Iikura, and H. Tanaka, "Applying a flexible microactuator to robotic mechanisms," *IEEE Control Systems Magazine*, vol. 12, no. 1, pp. 21–27, 1992.

[12] F. Connolly, P. Polygerinos, C. J. Walsh, and K. Bertoldi, "Mechanical programming of soft actuators by varying fiber angle," *Soft Robotics*, vol. 2, no. 1, pp. 26–32, 2015.

[13] L. Lin, F. Zhang, L. Yang, and Y. Fu, "Design and modeling of a hybrid soft-rigid hand exoskeleton for poststroke rehabilitation," *International Journal of Mechanical Sciences*, vol. 212, p. 106831, 2021.

[14] D. P. Holland, C. Abah, M. Velasco-Enriquez, M. Herman, G. J. Bennett, E. A. Vela, and C. J. Walsh, "The soft robotics toolkit: Strategies for overcoming obstacles to the wide dissemination of soft-robotic hardware," *IEEE Robotics & Automation Magazine*, vol. 24, no. 1, pp. 57–64, 2017.

[15] F. Schmitt, O. Piccin, L. Barbé, and B. Bayle, "Soft robots manufacturing: A review," *Frontiers in Robotics and AI*, vol. 5, p. 84, 2018.

[16] Programmable-Air. Last visited: 10-10-2022. [Online]. Available: https://www.programmableair.com/

[17] PneumaticBox CAPE - A system for real-time pneumatic control. Last visited: 10-10-2022. [Online]. Available: https://www.robotics.tu-berlin.de/menue/software_tutorials/pneumaticbox/

[18] Penuduino Toolkit. Last visited: 10-10-2022. [Online]. Available: http://pneuduino.org/toolkit/

[19] J. W. Booth, J. C. Case, E. L. White, D. S. Shah, and R. Kramer-Bottiglio, "An addressable pneumatic regulator for distributed control of soft robots," in *2018 IEEE International Conference on Soft Robotics (RoboSoft)*. IEEE, 2018, pp. 25–30.

[20] Y. Tian, R. Su, X. Wang, N. B. Altin, G. Fang, and C. C. Wang, "OpenPneu: Compact platform for pneumatic actuation with multi-channels," *arXiv preprint arXiv:2209.11318*, 2022.

[21] A. Shtarbanov, "FlowIO development platform–the pneumatic "Raspberry Pi" for soft robotics," in *Extended Abstracts of the 2021 CHI Conference on Human Factors in Computing Systems*, 2021, pp. 1–6.

[22] B. J. Caasenbrood, F. E. van Beek, H. K. Chu, and I. A. Kuling, "A desktop-sized platform for real-time control applications of pneumatic soft robots," in *2022 IEEE 5th International Conference on Soft Robotics (RoboSoft)*, 2022, pp. 217–223.

[23] T. R. Young, M. S. Xavier, Y. K. Yong, and A. J. Fleming, "A control and drive system for pneumatic soft robots: Pneusord," in *2021 IEEE/RSJ International Conference on Intelligent Robots and Systems (IROS)*. IEEE, 2021, pp. 2822–2829.

[24] C. D. Onal, X. Chen, G. M. Whitesides, and D. Rus, "Soft mobile robots with on-board chemical pressure generation," in *Robotics Research*. Springer, 2017, pp. 525–540.

[25] N. Napp, B. Araki, M. T. Tolley, R. Nagpal, and R. J. Wood, "Simple passive valves for addressable pneumatic actuation," in *2014 IEEE International Conference on Robotics and Automation (ICRA)*. IEEE, 2014, pp. 1440–1445.

[26] S. Wang, L. He, and P. Maiolino, "Design and characterization of a 3d-printed pneumatically-driven bistable valve with tunable characteristics," *IEEE Robotics and Automation Letters*, vol. 7, no. 1, pp. 112–119, 2022.

[27] D. C. Rucker and R. J. Webster III, "Statics and dynamics of continuum robots with general tendon routing and external loading," *IEEE Transactions on Robotics*, vol. 27, no. 6, pp. 1033–1044, 2011.

[28] C. Della Santina, R. K. Katzschmann, A. Bicchi, and D. Rus, "Model-based dynamic feedback control of a planar soft robot: Trajectory tracking and interaction with the environment," *The International Journal of Robotics Research*, vol. 39, no. 4, pp. 490–513, 2020.

[29] J. Till, V. Aloi, and C. Rucker, "Real-time dynamics of soft and continuum robots based on cosserat rod models," *The International Journal of Robotics Research*, vol. 38, no. 6, pp. 723–746, 2019.

[30] C. Duriez, "Control of elastic soft robots based on real-time finite element method," in *2013 IEEE International Conference on Robotics and Automation (ICRA)*, 2013, pp. 3982–3987.

[31] A. T. Mathew, I. M. B. Hmida, C. Armanini, F. Boyer, and F. Renda, "SoRoSim: A MATLAB toolbox for hybrid rigid-soft robots based on the geometric variable-strain approach," *IEEE Robotics Automation Magazine*, pp. 2–18, 2022.

[32] B. Caasenbrood, "Sorotoki - a soft robotics toolkit for MATLAB," https://github.com/BJCaasenbrood/SorotokiCode, 2020.

[33] Y. Yao, L. He, and P. Maiolino, "A simulation-based toolbox to expedite the digital design of bellow soft pneumatic actuators," in *2022 IEEE 5th International Conference on Soft Robotics (RoboSoft)*, 2022, pp. 29–34.

[34] S. Joshi and J. Paik, "Multi-DoF force characterization of soft actuators," *IEEE Robotics and Automation Letters*, vol. 4, no. 4, pp. 3679–3686, 2019.

[35] O. Fischer, Y. Toshimitsu, A. Kazemipour, and R. K. Katzschmann, "Dynamic task space control enables soft manipulators to perform real-world tasks," *Advanced Intelligent Systems*, p. 2200024, 2022.

[36] T. Ranzani, M. Cianchetti, G. Gerboni, I. D. Falco, and A. Menciassi, "A soft modular manipulator for minimally invasive surgery: Design and characterization of a single module," *IEEE Transactions on Robotics*, vol. 32, no. 1, pp. 187–200, 2016.

[37] J. Shi, W. Gaozhang, and H. A. Wurdemann, "Design and characterisation of cross-sectional geometries for soft robotic manipulators with fibre-reinforced chambers," in *2022 IEEE 5th International Conference on Soft Robotics (RoboSoft)*, 2022, pp. 125–131.

[38] K. Oliver-Butler, J. Till, and C. Rucker, "Continuum robot stiffness under external loads and prescribed tendon displacements," *IEEE Transactions on Robotics*, vol. 35, no. 2, pp. 403–419, 2019.

[39] G. Shi, A. Palombi, Z. Lim, A. Astolfi, A. Burani, S. Campagnini, F. G. Loizzo, M. L. Preti, A. M. Vargas, E. Peperoni *et al.*, "Fluidic haptic interface for mechano-tactile feedback," *IEEE transactions on Haptics*, vol. 13, no. 1, pp. 204–210, 2020.

[40] J. Fraś, J. Czarnowski, M. Maciaś, J. Główka, M. Cianchetti, and A. Menciassi, "New STIFF-FLOP module construction idea for improved actuation and sensing," in *2015 IEEE international conference on robotics and automation (ICRA)*. IEEE, 2015, pp. 2901–2906.

[41] A. Shariati, J. Shi, S. Spurgeon, and H. A. Wurdemann, "Dynamic modelling and visco-elastic parameter identification of a fibre-reinforced soft fluidic elastomer manipulator," in *2021 IEEE/RSJ International Conference on Intelligent Robots and Systems (IROS)*, 2021, pp. 661–667.